Multimed Tools Appl
DOI 10.1007/s11042-014-2092-1

Multipeak aniostropic microfacet model for iridescent surfaces

Young-Min Kang · Do-Hoon Lee · Hwan-Gue Cho

Received: 20 February 2014 / Accepted: 8 May 2014

Abstract In this paper, we propose an efficient iridescent rendering method. The iridescent colors on a surface is caused by the different reflection paths of rays with different wavelengths. In microfacet-based rendering model, the dominant reflection path of an incident light ray is statistically described by the microfacet-distribution function (MDF) of the surface. Therefore, the iridescent colors on the surface can be produced by applying different MDFs to different light wave channels. However, it is unnatural for a surface to have significantly different reflection properties in accordance with the light waves. Taking those into account, the proposed method employs identical and anisotropic microfacet distribution function(MDF) for each light wave channel, and rotates the identical anisotropic MDF of each channel with its own angle to produce iridescent reflection. The method also employs multi-peak MDF for the simulation of diffraction effects, and can be successfully applied to iridecent surface such as CD-ROM and mother-of-pearl (nacre) furniture. The experimental results demonstrate that the method enables interactive applications such as games or virtual reality softwares to plausibly express various cases of iridescent surfaces.

Keywords Rendering · Iridescent surface · Microfacet distribution

Y.-M. Kang (✉)
Department of Game Engineering, Tongmyong University, Sinseonno 428, Busan, Korea
e-mail: ymkang@tu.ac.kr

D.-H. Lee · H.-G. Cho
Department of Computer Engineering, Pusan National University, Busan, Korea

D.-H. Lee
e-mail: dohoon@pusan.ac.kr

H.-G. Cho
e-mail: hgcho@pusan.ac.kr

Published online: 01 June 2014

1 Introduction

Iridescent or goniochromatic surfaces such as shown in Fig. 1 are easily observed in everyday life. The iridescent reflection is caused by the fact that the rays of different wavelengths with an identical incident angle on the surface do not follow an identical reflection path. Four major mechanisms producing such iridescent colors are dispersive refraction (prism), scattering (rainbow), interference (oil slick), and diffraction (CD-ROMs) [1]. The iridescent phenomena by refraction and scattering were modeled earlier than those by interference and diffraction, and [13] is one of the earliest approaches in computer graphics literature. The effect of diffraction has long been left untouched in computer graphics society. In computer graphics literature, the effect of diffraction was first handled in [16], and the method was followed and improved by [1, 8, 17]. The most commonly accepted rendering equation is the one proposed in [9]. However, the equation only takes rays into account but not phase information [7]. The method proposed in [16] is based on the wave model proposed in [11]. The diffraction model was further improved in [7], and the iridescent phenomenon is now well modeled and represented in computer graphics applications. Musbach et al. simulated the propagation and reflection of electromagnetic waves, and the effect of interference and diffraction of light were incorporated in their simulation [12]. Although the previous methods successfully simulated goniochromatic effects caused by diffraction, their rendering models were too complex to be easily implemented especially in realtime applications. Therefore, we propose a simple microfacet-based model of which reflection properties can be easily manipulated. Despite the simplicity of the model, the method effectively and efficiently represents the iridescent surfaces.

Microfacet-based rendering was introduced by Torrance and Sparrow [18]. In this method, the surface was assumed as a collection of very small mirror-like facets, and the reflectance is determined by microfacet distribution function(MDF). Techniques for controlling the roughness of the surface were also introduced [4, 5], and those methods were also improved by Cook and Torrence [6]. In daily observation, we can easily notice that metallic surfaces show anisotropic reflectance because of the subtle normal perturbation on the surface. There have been various techniques for representing the anisotropic reflectance [14, 15, 19]. Ashikhmin and Shirley proposed an anisotropic reflection model with intuitive

(a) Photo of nacre furniture (b) Photo of CD-ROM

Fig. 1 Iridescent surfaces observed in real world: **a** mother-of-pearl furniture, **b** CD-ROM control parameters [2, 3]. Their model can be successfully utilized to express the surface with brushed scratches.

The method proposed in this paper exploits the anisotropic MDF and rotates the MDF for each color channel to produce the goniochromatic effect. In microfacet-based rendering model, the dominant reflection path of an incident light ray is statistically described by the MDF of the surface. Therefore, the iridescent colors on the surface can be produced by applying different MDFs to different light wave channels. However, it is unnatural for a surface to have significantly different reflection properties in accordance with the light waves. Taking those into account, the proposed method employs an identical and anisotropic MDF for each light wave channel, and rotates the identical anisotropic MDF of each channel with its own angle to produce iridescent reflection.

Because of the anisotropy of the base MDF, the rotated MDFs for light channels are different from each other and iridescent reflection can be easily obtained. In this paper, our goal is to propose an efficient rendering techniques for interactive applications which sometimes run on mobile platforms with limited resources. The microfacet model is widely accepted in realtime rendering techniques and well established. Therefore, the proposed method based on the microfacet model can be also implemented for such realtime or interactive applications.

2 Iridescent reflectance model

Microfacet model usually emplys an identical MDF regardless the wavelengths of incident light rays so that iridescent reflection cannot be obtained. In order to represent the iridescent surface, the MDF for each channel should be different from each other to reflect the rays with different wavelengths to different directions. Since the MDFs, however, represent the microscopic structure of the surface, it is natural that the MDFs should be similar to each other. In fact, we employed only one MDF for all the channels, and just changed the orientation of each MDF to obtain the goniochromatic effect. In other words, the rotated MDFs are identical in the aspect of the geometric shape but have different angular offsets to reflect rays with different wavelengths (in our method, rays in different channels) to the different directions.

Since the rotated MDFs should not be identical to each other, the original MDF must be anisotropic. Therefore, we employed anisotropic MDFs to model the iridescent reflection surface. The reflectance property of microfacet-based surface model is determined by the MDF $D(\omega_h)$ which gives the probability that a microfacet is oriented to the direction ω_h. Many researchers have proposed various anisotropic reflection models [2, 3, 19], and any of the models can be easily employed for our model. The MDF of the aniostropic bidirectional reflectance distribution function proposed by Ashikhmin and Shirley is described as follows [2, 3]:

$$D(\omega_h) = \frac{\sqrt{(e_x+1)(e_y+1)}}{2\pi}(\omega_h \cdot \mathbf{n})^{e_x \cos^2\phi + e_y \sin^2\phi}, \tag{1}$$

where $\mathbf{n}$ is the normal vector at the point to be rendered.

The actual parameter ω_h in the MDF is the half way vector between the incident light direction and outgoing viewing direction. e_x and e_y are parameters that control the anisotropy of the reflection, and ϕ is the azimuthal angle. ω_h is a unit vector which is sufficiently represented with only two components as $(\omega_h.x, \omega_h.y, \sqrt{1-\omega_h.x^2-\omega_h.y^2})$.

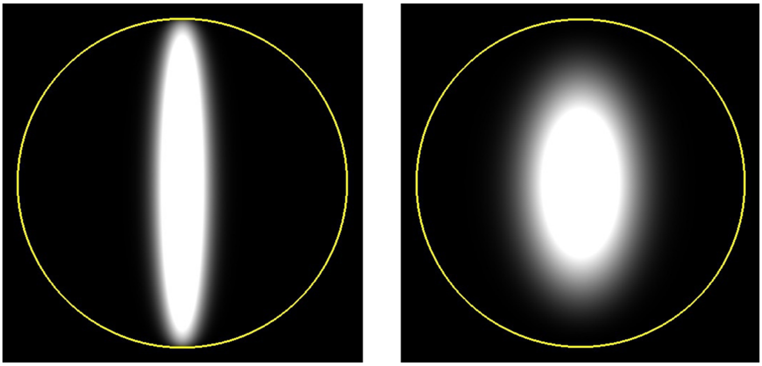

(a) $e_x = 100, e_y = 1$ (b) $e_x = 20, e_y = 5$

Fig. 2 MDF in 2D space

Therefore the MDF is also defined in 2D space as shown in Fig. 2, and the half vector ω_h can be regarded a 2-dimensional projected vector by ignoring the z-component (i.e., $\omega_h \in \mathcal{R}^2$).

Figure 2 shows an example of anisotropic MDF using (2) with different e_x and e_y. As shown in Fig. 2, the incoming light energy is scattered differently in x(tangent) and y(binormal) axes of tangent space.

We employed standard RGB model instead of full-range wave model in order to efficiently render the surface. The original MDF as shown in Fig. 2 is used only for the R-channel, and the orginal MDF is rotated around the center of the MDF domain space with angles θ_1 and θ_2. The rotated MDF with angle θ_1 is used for the G-channel, and the other with θ_2 is for the B-channel.

Figure 3 shows the per-channel rotated MDFs shown in Fig. 2 with $\theta_1 = 0.2$ and $\theta_2 = 0.4$. It is the matter of course that the actual rotation of the MDF function is only a conceptual process. Instead, we simply compute the per-channel intensity with different half vectors for each channel. Suppose that the half vector is given as ω_h and let us denote the half vector for each channel as ω_h^r, ω_h^g and ω_h^b respectively.

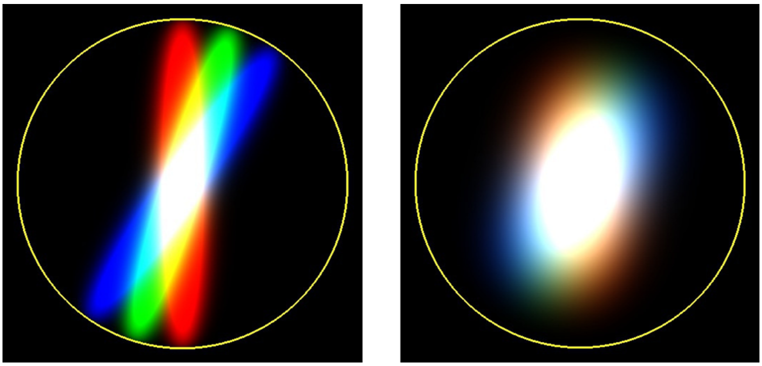

(a) $e_x = 100, e_y = 1$ (b) $e_x = 20, e_y = 5$

Fig. 3 Ashikhmin MDF rotated with $\theta_1 = 0.2$ and $\theta_2 = 0.4$

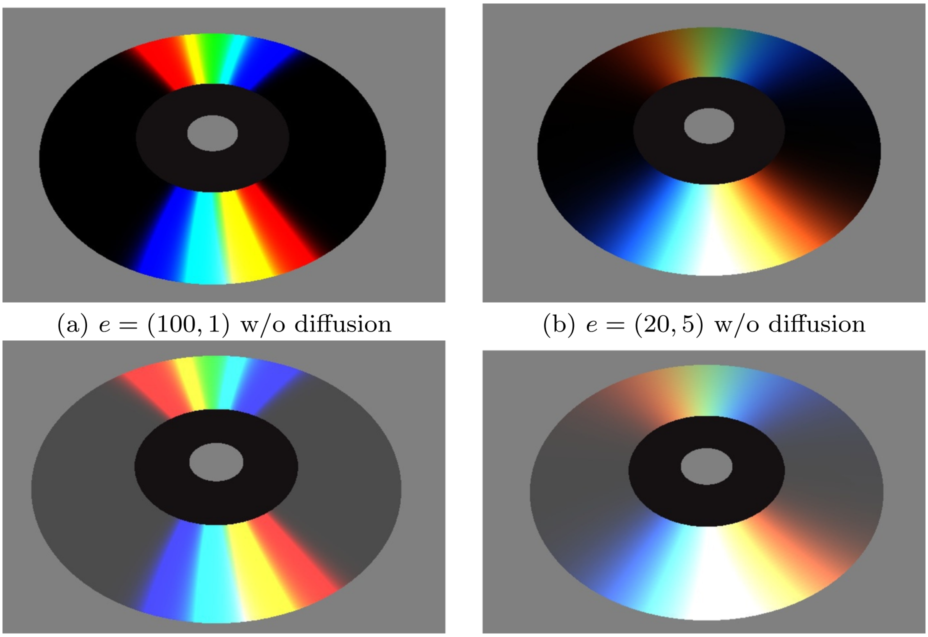

(a) $e = (100, 1)$ w/o diffusion

(b) $e = (20, 5)$ w/o diffusion

(a) $e = (100, 1)$ + diffusion

(b) $e = (20, 5)$ + diffusion

Fig. 4 CD-ROM rendering with rotated Ashikhmin MDFs

It is obvious that generating the rotated MDF for each channel by explicitly rotating the values of the distribution function is too expensive. In the actual rendering process, we obtain the reflection of the rotated MDF by simply rotate the half vectors employed in the computation. Let us denote by $\mathbf{R}_\theta$ the 2×2 matrix that rotates 2-dimensional vectors through an angle θ about the origin of the Cartesian coordinate system of the MDF domain. The half vectors for each channel, then, can be easily computed as follows:

$$\begin{aligned} \omega_h^r &= \omega_h \\ \omega_h^g &= \mathbf{R}_{\theta_1} \omega_h \\ \omega_h^b &= \mathbf{R}_{\theta_2} \omega_h \end{aligned} \tag{2}$$

In order to verify the iridescent reflection property of the rotated MDFs, we applied the MDFs shown in Fig. 3 to a CD-ROM model, and obtained the rendering results as shown in Fig. 4. The first row shows the reflection without diffuse components while the other row shows rendering with some diffuse reflection. The results shown in the first column are rendered with the MDF shown in Fig. 3a, and the others are with the one shown in Fig. 3b. As shown in the figure, the per-channel rotation of anisotropic MDF produced iridescent reflection on the surface.

3 Simulating diffraction effects

Although the simple rotation of anisotropic MDFs can show iridescent reflection as shown in the previous section, the actual iridescent phenomenon is more complicated. Physically speaking, the iridescent reflection on CD-ROMs are because of the diffraction and interference of light waves. It is also well known that the reflected light waves undergone the diffraction and the interference do not produce single specular intensity pattern, but produce multiple specular intensity pattern because of the interference [12].

However, the usual MDFs such as those for Ashikhmin's BRDF or Ward's BRDF have only one specular peak so that it is impossible to represent the multiple specular reflection by interference. In oder to easily simulate the interference of light waves, we employed multipeak MDFs for the iridescent surfaces.

It is natural for an MDF to have the highest value at the center of the domain space and the multipeak specular reflection should be observed periodically along the diameters of the circular MDF domain. Such concentric multipeak patterns can be easily modeled with trigonometric functions. Let us denote by r the distance between the center of the 2-dimensional MDF domain and the half vector ω_h is the halfway vector projected on the domain space (i.e., $\sqrt{\omega_h.x^2 + \omega_h.y^2}$). The concentric multipeak pattern can then be expressed as $\frac{1}{2}(\cos 2\pi\mu_f r + 1)$ where μ_f is the frequency of the wave. Because normal vectors are obviously concentrated near the center of the MDF, it is natural that the mutipeak patterns attenuate as the distance from the center increases. Such an attenuation can be simply modeled by multiplying the dot product of the normal vector and the half vector to the peoridic multipeak patterns. This idea is visualized in Fig. 5 where the periodic wave function is multiplied by $(\mathbf{n} \cdot \omega_h)$. Therefore, the multipeak MDF can be easily modeled with a control parameter μ_f for the number of peaks as follows:

$$\begin{aligned} r &= \sqrt{\omega_h.x^2 + \omega_h.y^2} \\ D(\omega_h) &= \frac{1}{2}(\mathbf{n} \cdot \omega_h)(\cos 2\pi\mu_f r + 1) \end{aligned} \tag{3}$$

The MDF shown in (3) has multiple specular peaks in accordance with the parameter μ_f, and the specular intensity decreases as the half vector approaches to the circumference of the

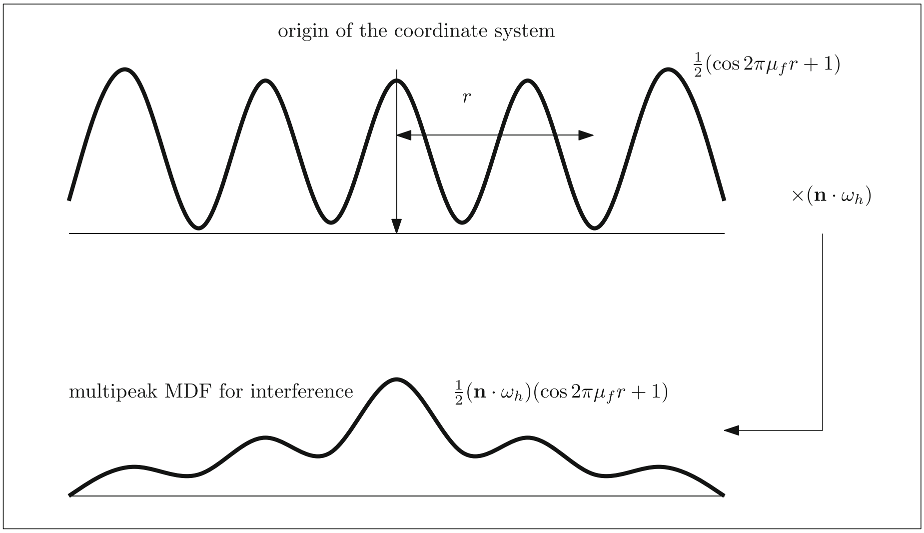

Fig. 5 Multipeak reflection model for interference representation

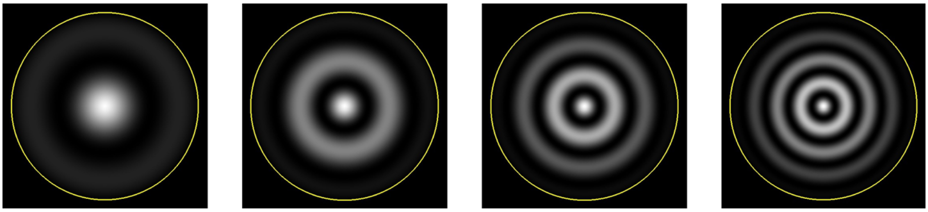

(a) $\mu_f = 1$ (a) $\mu_f = 2$ (a) $\mu_f = 3$ (a) $\mu_f = 4$

Fig. 6 Multipeak specular MDF with different μ_f values

MDF domain space. The resulting MDFs with different μ_f values are shown in Fig. 6. The iridescent colors can be obtained only when the MDFs for different channels are different from each other. However, the multipeak MDFs generated with (3) are all isotropic and the rotated ones are identical with the original MDF. In other words, the iridescent surface rendering method proposed in this paper cannot be applied to the multipeak MDFs shown in Fig. 6. Therefore, we transformed the MDFs to be anisotropic by employing anisotropy control parameters α and β as follows:

$$\begin{aligned} r &= \sqrt{\alpha\omega_h.x^2 + \beta\omega_h.y^2} \\ D(\omega_h) &= \frac{1}{2}(\mathbf{n}\cdot\omega_h)(\cos\mu_f 2\pi r + 1) \end{aligned} \tag{4}$$

By applying $\alpha = 1$ and $\beta = 0.1$, the MDFs shown in Fig. 6 are transformed as shown in Fig. 7. The anisotropic MDFs generated with different α and β values can then be easily utilized for the MDF rotation method described in the previous section.

4 Experiments

The rotated MDFs with various control parameters and the CD-ROM rendered with the MDFs are shown in Fig. 8. The multipeak reflection property of the proposed MDF model makes it possible to produce more natural diffraction effect than the those produced with the simple rotation of single peak MDFs. As shown in the figure, the proposed method can efficiently control the diffraction and interference pattern with simple control parameters and the implementation of the proposed method is as easy as conventional MDF-based realtime rendering techniques.

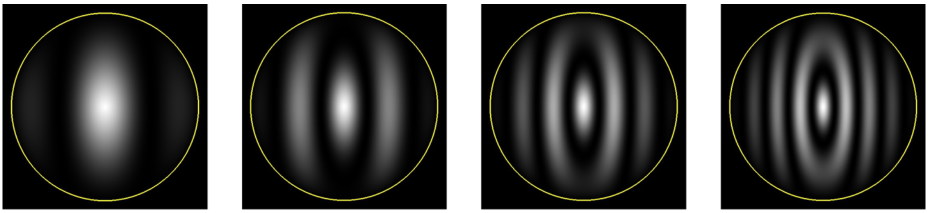

(a) $\mu_f = 1$ (a) $\mu_f = 2$ (a) $\mu_f = 3$ (a) $\mu_f = 4$

Fig. 7 Anisotropic multipeak MDFs with $\alpha = 1$ and $\beta = 0.1$

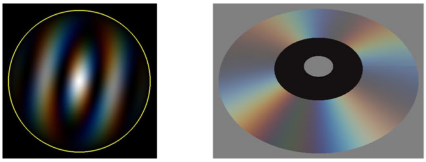

(a) $\mu_f = 2, \alpha = 1, \beta = 0.1, \theta_1 = 0.2, \theta_2 = 0.4$

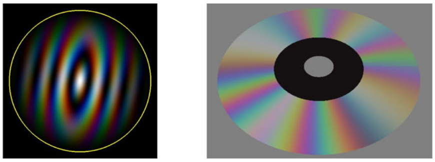

(b) $\mu_f = 4, \alpha = 1, \beta = 0.1, \theta_1 = 0.2, \theta_2 = 0.4$

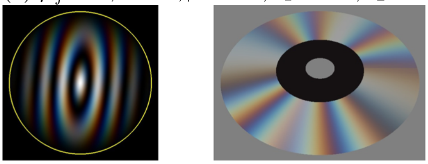

(c) $\mu_f = 4, \alpha = 1, \beta = 0.1, \theta_1 = 0.1, \theta_2 = 0.2$

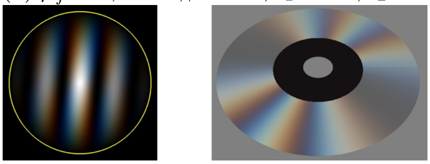

(d) $\mu_f = 2, \alpha = 1, \beta = 0, \theta_1 = 0.1, \theta_2 = 0.2$

Fig. 8 Rotated anisotropic multipeak MDFs and the corresponding CD-ROM rendering results

Figure 9 compares the photos of real CD-ROMs and virtual CD-ROMs rendered with the proposed method. The previous methods for iridescent reflection on optical disks generate straight strips on the disk. However, the actual optical disks show curved strips as shown in the upper row of the figure. The method proposed in this method can plausibly generate

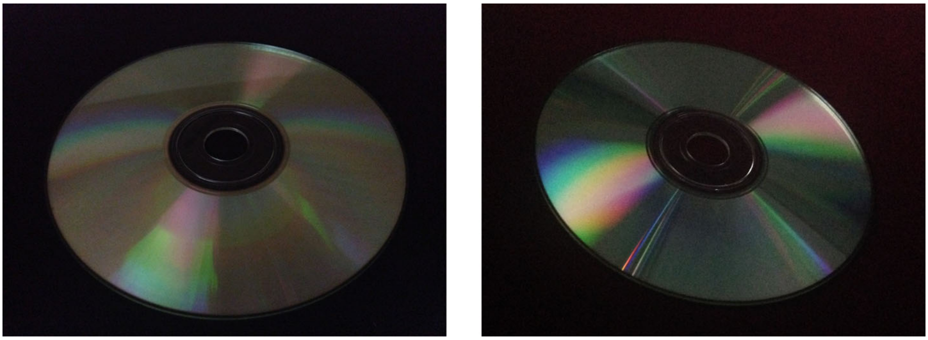

(a) real CD-ROMs

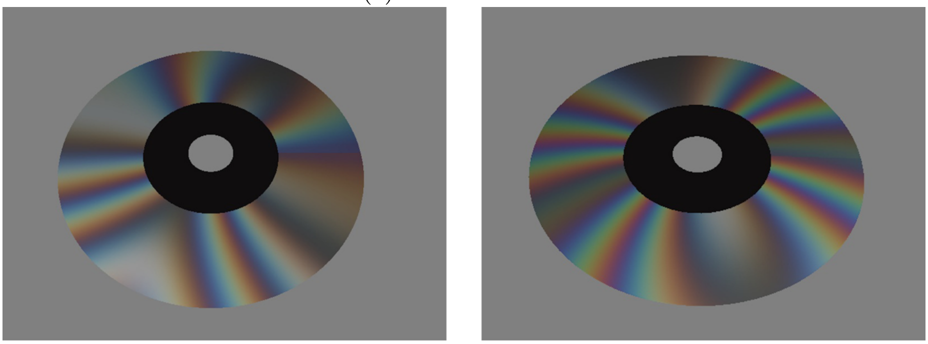

(b) simulated CD-ROMs

Fig. 9 Comparison between real CD-ROM photo and simulated iridescent reflection on a virtual CD-ROM **a** real CD-ROM, **b** simulated CD-ROM (parameter settings: $\mu_f = 8.5, \alpha = 2.0, \beta = 1.2, \theta_1 = 0.1, \theta_2 = 0.2$ and $\mu_f = 2.5, \alpha = 1.0, \beta = 5.0, \theta_1 = 0.1, \theta_2 = 0.2$ respectively)

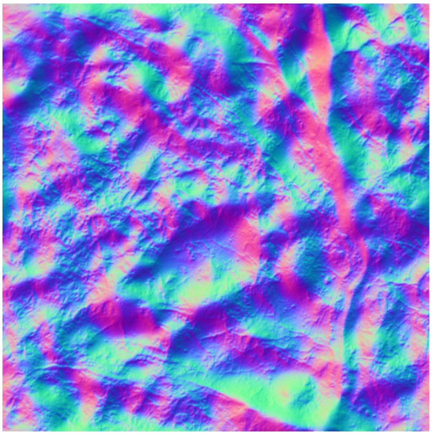

(a) Normal map

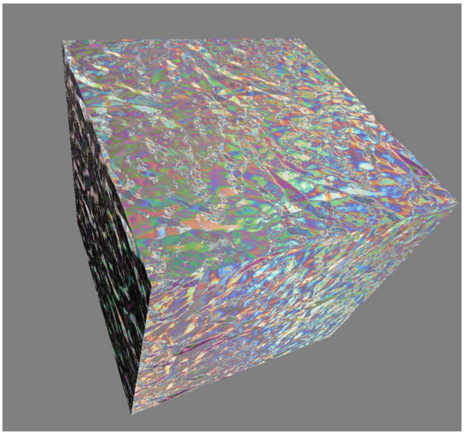

(b) $\mu_f = 2, \theta_1 = 0.3,\ \theta_2 = 0.6$

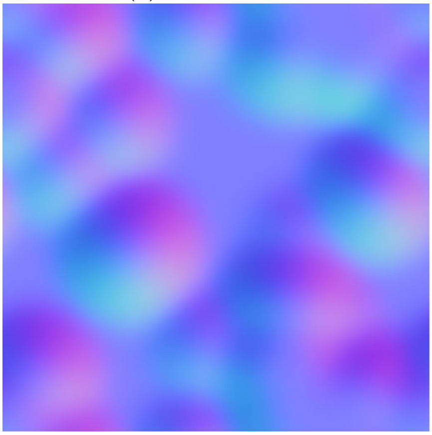

(c) Nacre normal map

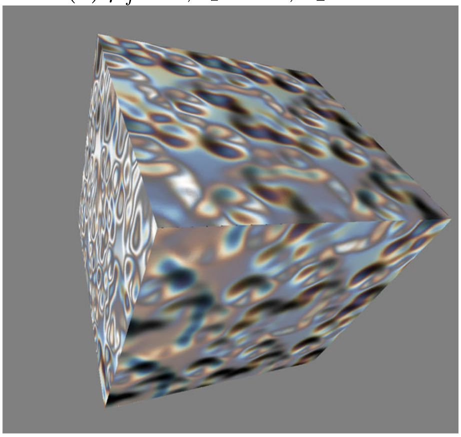

(d) $\mu_f = 3, \theta_1 = 0.1,\ \theta_2 = 0.2$

Fig. 10 Iridescent surfaces with perturbed normals ($\alpha = 1$, $\beta = 0.1$)

the curved strips as shown in the lower row in the figure. The parameter settings for two simulated CD-ROMs in the lower row are ($\mu_f = 8.5, \alpha = 2.0, \beta = 1.2, \theta_1 = 0.1, \theta_2 = 0.2$) and ($\mu_f = 2.5, \alpha = 1.0, \beta = 5.0, \theta_1 = 0.1, \theta_2 = 0.2$) respectively.

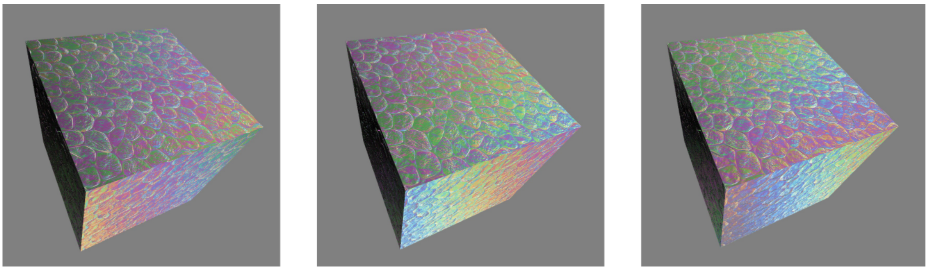

Fig. 11 Iridescent colors with different incident lights

Fig. 12 Photo of an inlaid mother-of-pearl box housed in the Los Angeles County Museum of Art [10]

Since our method is based on the microfacet model, the normal vectors on the surface play very important role in producing the iridescent colors. Therefore, various iridescent reflection effects can be easily generated by simply perturbing the normals. The proposed method was applied to a surface with normals perturbed with the normal map in order to verify the iridescent reflection of the method. Figure 10a is the normal map to perturb the surface normals, and (b) is the rendered cube with the perturbed normals. The control parameters are $\mu_f = 2, \alpha = 1, \beta = 0.1, \theta_1 = 0.3$, and $\theta_2 = 0.6$. To demonstrate the effectiveness of the proposed methods, we exploited the method to represent the iridescent reflection of nacre (i.e., mother of pearl). The iridescent reflection on the nacre is known to be caused by diffraction and interference. However, the full simulation of the diffraction and interference is difficult to model and requires heavy computational overheads. We

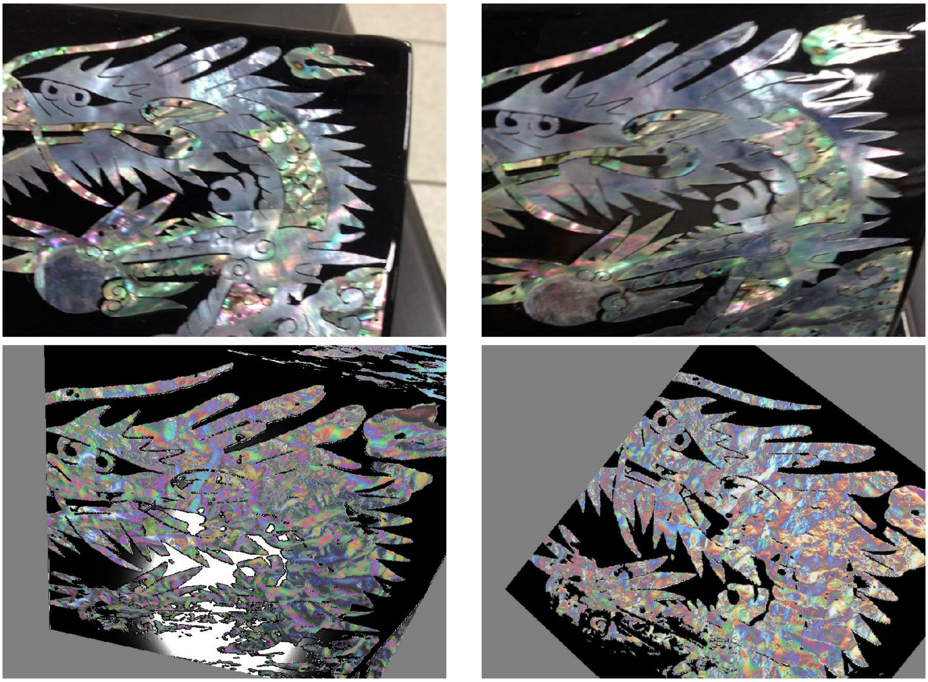

Fig. 13 Comparision between real nacre furniture (*upper*) and simulated one (*lower*)

found such an iridenscent reflection can be easily represented by our method. The normal perturbation for the mother of pearl is performed with the normal map shown in Fig. 10c, and the nacre-like surface was produced as shown in (d).

Figure 11 shows the iridescent reflection on the surface with an identical normal map and different incident lights. As shown in the figure, the method proposed in this paper can effectively and efficiently express the goniochromatic surface.

The mother-of-pearl objects were widely used for decorating the furnitures in East Asia, especially in Korea. Figure 12 is the photo of an inlaid mother-of-pearl box which is housed in the Los Angeles Count Museum of Art. The method proposed in this paper can be easily employed to express the iridescent reflection of the mother-of-pearl as shown in such furnitures.

We used the nacre model to represent real objects such as ‘mother-of-pearl furniture’ as shown in Fig. 13. In the figure, the real nacre furniture and simulated one are compared. The control parameters for iridescent reflection are identically specified for all the models. The upper row shows the photos of real nacre furniture and the lower row shows the simulated one. As shown in the figure the proposed method could express plausible nacre

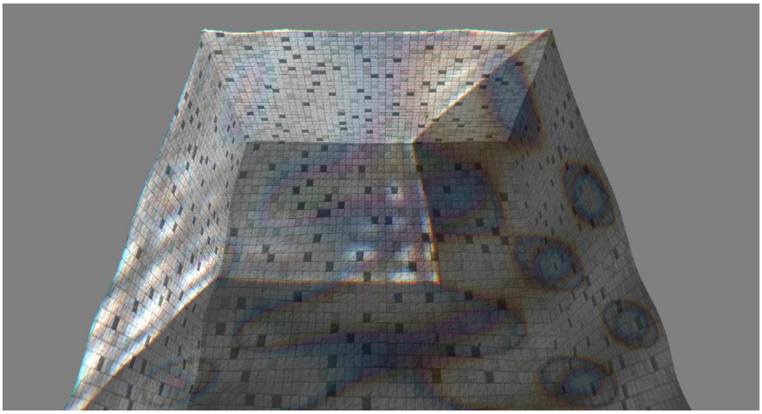

(a) $\mu_f = 10 \alpha = 20, \beta = 1, \theta_1 = 0.1, \theta_2 = 0.2$

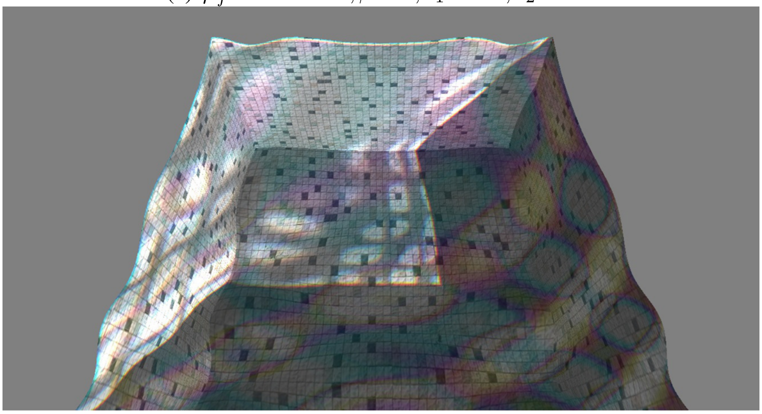

(a) $\mu_f = 3 \alpha = 2, \beta = 1, \theta_1 = \pi/6, \theta_2 = \pi/3$

Fig. 14 Rendered iridescent liquid surface like water covered oil slick furniture reflection although the whole part of the virtual nacre in the simulated one is represented with an identical control parameter setting and the actual nacre decoration in the real furniture is composed of nacre parts with different reflection properties.

We also applied our method to a different iridescent phenonemon which is caused by light interference. The method could plausibly express the interference of the light reflected on oil slick as shown in Fig. 14. The water covered with oil shown in the top of the figure is generated with the parameters $\mu_f = 10\alpha = 20, \beta = 1, \theta_1 = 0.1, \theta_2 = 0.2$ and the other shown in the bottom is with $\mu_f = 3\alpha = 2, \beta = 1, \theta_1 = \pi/6, \theta_2 = \pi/3$. As shown in the figure, our method successfully expressed the light interference on the oil slick.

5 Conclusion

In this paper, we proposed an efficient iridescent rendering method based on microfacet model. There have been various efforts to model the iridescent reflection in computer graphics literature. However, the previous methods tried to simulate the actual light wave transportation so that the rendering models were unnecessarily difficult. The method proposed in this paper employs the standard RGB-channel model and microfacet reflection model which are commonly accepted in computer graphics literature, especially in real-time rendering area. The method simply rotates the anisotropic microfacet distribution in the MDF domain space to represent the iridescent phenomenon, and employs multi-peak MDF for the simulation of diffraction effects. The rotated anisotropy of the base MDF made it possible for rays in different channels travel in different paths, and the multi-peak MDF model produced subtle light reflection similar to the actual light interference of light waves after the diffraction. Therefore, the method proposed in this paper can be successfully applied to iridecent surface such as CD-ROM and mother-of-pearl. Since the method is based on easily implementable and widely accepted MDF-based RGB model, it is very efficient, straighforwardly understood and easily implemented.

References

1. Agu E, Hill FS Jr (2002) Diffraction shading models for iridescent surfaces. In: Proceedings of IASTED VIIP
2. Ashikhmin M, Premoze S, Shirley P (2000) A microfacet-based brdf generator. In: Proceedings of ACM SIGGRAPH 2000, pp 65–74
3. Ashikhmin M, Shirley P (2002) An anisotropic phong brdf model. J Graphics Tools 5(2):25–32
4. Blinn J (1977) Models of light reflection for computer synthesized pictures. In: Proceedings of the 4th annual conference on computer graphics and interactive techniques, pp 192–198
5. Blinn J, Newell M (1976) Texture and reflection in computer generated images. Commun ACM 19(10):542–547
6. Cook RL, Torrance KE (1981) A reflectance model for computer graphics. Comput Graph (ACM Siggraph '81 Conference Proceedings) 15(3):307–316

7. Cuypers T, Haber T, Bekaert P, Oh SB, Raskar R (2012) 5. ACM Trans Graph 31:122:1–122:11. doi:10.1145/2231816.2231820
8. Hirayama H, Yamaji Y, Kaneda K, Yamashita H, Monden Y (2000) Rendering iridescent colors appearing on natural objects. In: Proceedings of the eighth pacific conference on computer graphics and applications 2000, pp 15–22
9. Kajiya JT (1986) The rendering equation. In: ACM SIGGRAPH Computer Graphics, vol 20, pp 143–150. ACM
10. LACMA: Black-lacquered wardrobe chest with peony and arabesque design (2013). http://collections.lacma.org/node/199634
11. Moravec HP (1981) 3d graphics and the wave theory. In: ACM SIGGRAPH computer graphics, vol 15, pp 289–296. ACM
12. Musbach A, Meyer GW, Reitich F, Oh SH (2013) Full wave modeling of light propagation and reflection. Comput Graph Forum 32(6):24–37
13. Musgrave FK (1989) Prisms and rainbows: a dispersion model for computer graphics. In: Proceedings of graphics interface, vol 89, pp 227–234
14. Poulin M, Founier A (1990) A model for anisotropic reflection. Comput Graph (ACM Siggraph ’90 Conference Proceedings) 23(4):273–282
15. Schilick C (1993) A customizable reflectance model for everyday rendering. In: Proceedings of the 4th Eurographics workshop on rendering, pp 73–84
16. Stam J (1999) Diffraction shaders. In: Proceedings of the 26th annual conference on computer graphics and interactive techniques, SIGGRAPH ’99. ACM Press/Addison-Wesley Publishing Co., New York, pp 101–110. doi:10.1145/311535.311546
17. Sun Y, Fracchia FD, Drew MS, Calvert TW (2000) Rendering iridescent colors of optical disks. In: Proceedings of rendering techniques ’00, pp 341–352. Springer
18. Torrance KE, Sparrow EM (1967) Theory for off-specular reflection from roughened surfaces. J Opt Soc Am 57(9):1105–1112
19. Ward G (1992) Measuring and modeling anisotropic reflection. Comput Graph (ACM Siggraph ’92 Conference Proceedings) 26(2):265–272

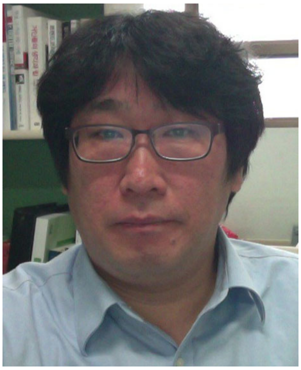

Young-Min Kang received his B.S., M.S.(1999), and Ph.D.(2003) degrees from Pusan National University. He was a temporary researcher at MIRALab in University of Geneva and worked as a researcher at Electronics and Telecommunication Research Institute (ETRI), Korea. His research interests include physically based animation, realtime rendering, general purpose GPU programming and game programming. He is currently an associate professor at the Game Engineering Department in Tongmyong University, Korea.

Do-Hoon Lee received his B.S.(1986), M.S.(1992), and Ph.D.(1998) degrees from Pusan National University, Korea. He worked at Computer Engineering Department in Miryang National University, Korea from 1995 to 2005. He was a visiting scholar at School of Informatics of Indiana University at Bloomington, Indiana from 2004 to 2006. He has been a faculty member in Pusan National University since March 2006. His research interests include UI/UX/BCI, computer graphics, the analysis of RNA-seq data in bioinformatics and integrated and computational network modeling of biomedical informatics.

Hwan-Gue Cho received his B.S. degree(1984) from Seoul National University and the M.S. and Ph.D.(1990) degrees from Korea Advanced Institute of Science and Technology, Korea. Since 1990 he has been a Professor in Pusan National University, Korea. His research interests include visualization and bioinformatics (especially on sequence alignment and biological network analysis). Recently he works on machine learning algorithm for characterizing network structure on interaction among general objects.